Theory of tetragonal twin structures in ferroelectric perovskites with a first-order phase transition

Wenwu Cao and L. E. Cross
Materials Research Laboratory, The Pennsylvania State University, University Park, Pennsylvania 16802
(Received 11 February 1991)

A three-dimensional Landau-Ginzburg model has been constructed to describe the tetragonal twin structures resulting from a first-order O_h-C_{4v} proper ferroelectric phase transition in perovskites. The model takes into account the nonlinear and nonlocal characteristics of the polarization (order parameter) as well as the electromechanical coupling. Quasi-one-dimensional (Q1D) analytic solutions for the space profiles of the order parameter are obtained for a 180° twin and for a charge-neutral 90° twin with a special choice of parameters. Without the presence of interfacial defects, such as dislocations, the Q1D solutions require the support of inhomogeneous mechanical constraints. Elastic deformation and dimensional changes associated with the twin structures, and their implications on the piezoelectric effect in ferroelectric ceramics, are also addressed.

I. INTRODUCTION

Many important ferroelectric materials, such as $PbTiO_3$, $BaTiO_3$, $(Pb_{1-x}Zr_x)TiO_3$ [PZT], etc., have perovskite structure (ABX_3).[1] The prototype phase is cubic with symmetry group O_h, which transforms to a ferroelectric tetragonal (C_{4v}) or rhombohedral (C_{3v}) structure upon cooling. In certain materials there are several low-temperature ferroelectric phases, so that the stable structure of a material depends on the given temperature range.

These thermally induced structural phase transitions are usually displacive, and there are several low-temperature variants associated with each phase transition. For instance, there are six and eight variants in the tetragonal and rhombohedral phases, respectively, upon transforming from cubic. These variants are energetically equivalent; therefore, twinning between these variants is a common phenomenon under natural conditions. For single crystals with free boundary conditions, twinning may be eliminated through (electric or mechanical) field-induced domain switching between these low-temperature variants. However, twinning cannot be eliminated for a confined system, such as grains in a ceramic, because unit-cell distortions are usually associated with these ferroelectric transitions, domain switching could generate large elastic energy. Although, for some materials, a single phase may be achieved under a very large electric field, twinning will reappear when the external field is removed in order to release some of the elastic strain so as to minimize the total system energy. For other materials, twinning cannot be driven out by the electric field before the solid is shattered.

The existence of these twinning structures often changes the mechanical and electrical properties of a ferroelectric material substantially. There are considerable experimental studies being carried out in this regard[2,3] and some phenomenological theories were also developed.[4–6] However, in order to understand the physical process associated with the twinning phenomenon, one has to go down to the microscopic level to see how the lattices move in forming a twin structure and how they interact with each other. To this end, it is essential to know the structure of a twin boundary, including its stable space profile, energy density, and associated elastic distortions. In this paper, we will calculate these physical properties for a ferroelectric twin boundary by using a Landau-Ginzburg type of continuum theory. The problem we are dealing with is a first-order cubic to tetragonal proper ferroelectric transition, which appears in systems such as $BaTiO_3$, $PbTiO_3$, and some PZT compositions.

There are six tetragonal variants upon transforming from cubic; they can form three different kinds of twinning structures: (1) 180° twins, for which the polarizations in the two domains have the same magnitude but in opposite directions, (2) 90° twin with a charge-neutral domain wall, for which the polarizations in the two domains are (almost) perpendicular to each other with head to tail configuration, and (3) 90° twin with a charged domain wall, for which the polarizations in the two domains are perpendicular to each other and with either head-to-head or tail-to-tail configurations. It has been verified that the third kind of twin structure is unstable and will transform into the second kind with a zigzag twin boundary.[7]

Several authors[8–10] have attempted to model the structure of ferroelectric domain walls by using the Landau-Ginzburg theory; however, those models are either one dimensional or three dimensional with gradient terms in the free-energy expansion not obeying the symmetry requirement. Moreover, the focusing point was on the first kind (180°) of twins only. It has been pointed out that a one-dimensional model is not adequate for describing a three-dimensional solid.[11] A quasi-one-dimensional (Q1D) solution can be obtained only under certain constraints when unit-cell distortions are involved. We have taken all of these points into account in our three-dimensional model described in this paper, which can give a full description of both the first and the second

kind of domain walls mentioned above. Analytic expressions of the order-parameter profiles for a 180° twin and a 90° twin were derived, although special parameters were chosen in order to get the 90° twin solution. The boundary conditions and the associated shape change were also addressed in our model. The expansion coefficients in the free-energy equation (2.1) can be determined experimentally, which enables one to apply the present model to a real system.[12]

This paper is divided into six sections. We introduce the theoretical model in Sec. II. Sections III–V are the solutions for the tetragonal phase with a homogeneous structure, 180° twin, and 90° twin, respectively. Section VI contains the summary and conclusions.

II. THEORETICAL MODEL

The order parameter for describing the O_h-C_{4v} proper ferroelectric phase transition is the polarization vector **P**. The free-energy density, which is invariant under O_h symmetry, can be written as

$$F(P_i,P_{i,j},\eta_{kl})=F_L(P_i)+F_{\rm el}(\eta_{kl})+F_c(P_i,\eta_{kl})+F_G(P_{i,j}) . \tag{2.1}$$

We should emphasize here that **P** is the material measure of polarization which ensures the invariant nature of the free energy.[13] The first term in Eq. (2.1) is the Landau-Devonshire free energy:

$$F_L(P_i)=\alpha_1(P_1^2+P_2^2+P_3^2)+\alpha_{11}(P_1^2+P_2^2+P_3^2)^2+\alpha_{12}(P_1^2P_2^2+P_2^2P_3^2+P_1^2P_3^2)+\alpha_{111}(P_1^6+P_2^6+P_3^6)$$
$$+\alpha_{112}[P_1^4(P_2^2+P_3^2)+P_2^4(P_1^2+P_3^2)+P_3^4(P_1^2+P_2^2)]+\alpha_{123}P_1^2P_2^2P_3^2 , \tag{2.2}$$

where α_{11} is negative for describing a first-order transition. The second term in Eq. (2.1) is the elastic energy of the system,

$$F_{\rm el}(\eta_{kl})=\frac{C_{11}}{2}(\eta_{11}^2+\eta_{22}^2+\eta_{33}^2)+C_{12}(\eta_{11}\eta_{22}+\eta_{11}\eta_{33}+\eta_{22}\eta_{33})+2C_{44}(\eta_{12}^2+\eta_{13}^2+\eta_{23}^2) . \tag{2.3}$$

$\eta_{kl}=\frac{1}{2}(u_{k,l}+u_{l,k})$ $(k,l=1,2,3)$ is the linear elastic strain tensor which serves as a secondary order parameter here, u_k is the component of elastic displacement, C_{ij} are the second-order elastic constants. The third term in Eq. (2.1) represents the coupling between the primary and the secondary order parameters:

$$F_c(P_i,\eta_{kl})=-q_{11}(\eta_{11}P_1^2+\eta_{22}P_2^2+\eta_{33}P_3^2)-q_{12}[\eta_{11}(P_2^2+P_3^2)+\eta_{22}(P_1^2+P_3^2)+\eta_{33}(P_1^2+P_2^2)]$$
$$-2q_{44}(\eta_{12}P_1P_2+\eta_{13}P_1P_3+\eta_{23}P_2P_3) , \tag{2.4}$$

q_{ij} are the electrostrictive constants. The fourth term in Eq. (2.1) is the gradient energy of the lowest-order compatible with the cubic symmetry, which has the invariant form

$$F_G(P_{i,j})=\tfrac{1}{2}g_{11}(P_{1,1}^2+P_{2,2}^2+P_{3,3}^2)+g_{12}(P_{1,1}P_{2,2}+P_{1,1}P_{3,3}+P_{2,2}P_{3,3})$$
$$+\frac{g_{44}}{2}[(P_{1,2}+P_{2,1})^2+(P_{1,3}+P_{3,1})^2+(P_{2,3}+P_{3,2})^2] . \tag{2.5}$$

All the expansion coefficients in Eqs. (2.2)–(2.5) are assumed to be independent of temperature except α_1 in Eq. (2.2), which signifies that the transition is proper ferroelectric.

For convenience we define the following new constants:

$$\hat{C}_{11}=C_{11}+2C_{12} , \tag{2.6a}$$

$$\hat{C}_{22}=C_{11}-C_{12} , \tag{2.6b}$$

$$\hat{q}_{11}=q_{11}+2q_{12} , \tag{2.7a}$$

$$\hat{q}_{22}=q_{11}-q_{12} . \tag{2.7b}$$

They are the bulk and shear elastic constants and electrostrictive constants, respectively.

III. STATIC EQUILIBRIUM CONDITIONS AND THE HOMOGENEOUS SOLUTIONS

The static equilibrium conditions can be derived from the total energy expansion by using variational method, which gives rise to the Euler equations for the primary and secondary order parameters:

$$\frac{\partial}{\partial x_j}\left[\frac{\partial F}{\partial P_{i,j}}\right]-\frac{\partial F}{\partial P_i}=0 \quad (i,j=1,2,3) , \tag{3.1}$$

$$\sigma_{ij,j}^{\rm tot}=\frac{\partial}{\partial x_j}\left[\frac{\partial F}{\partial \eta_{ij}}\right]=0 \quad (i,j=1,2,3) . \tag{3.2}$$

The Cauchy stress tensor $\sigma_{ij}^{\rm tot}$ includes contributions from the pure elastic response and the electrostrictive effect.

In order to avoid the complication of defects, we only consider the case for which no dislocations and disclinations are generated in the structural phase transition, which means that the following compatibility relations[14] must also be satisfied:

$$\epsilon_{ikl}\epsilon_{jmn}\eta_{ln,km}=0 \quad (i,j,k,l,m,n=1,2,3) , \tag{3.3}$$

where ϵ_{ikl} is the permutation symbol (or Levi-Civita density).

For a homogeneous system, all physical quantities are uniform in space, hence, Eq. (3.3) becomes trivial and Eqs. (3.1) and (3.2) reduce to the following simple equations:

$$\frac{\partial F}{\partial P_i}=0 , \tag{3.4}$$

$$\sigma_{ij}^{\text{tot}}=\text{const}=0 . \tag{3.5}$$

We have set the constant in Eq. (3.5) to zero, assuming that the system being studied is free of external stresses.

Equations (3.4) and (3.5) can be easily solved, there are four different temperature ranges which we will discuss separately. It is customary to assume that α_1 depends linearly on temperature, i.e., $\alpha_1=\alpha_0(T-T_0)$, where α_0 is positive definite, then the solutions for the homogeneous system are the following.

(i) For $T>T_1$ where

$$T_1=T_0+\frac{{\alpha'_{11}}^2}{3\alpha_0\alpha_{111}} ,$$

$$\alpha'_{11}=\alpha_{11}-\frac{q_{11}^2}{6\hat{C}_{11}}-\frac{\hat{q}_{22}^2}{3\hat{C}_{22}} ,$$

$$P_i=0, \quad \eta_{ij}=0 \quad (i,j=1,2,3) , \tag{3.6}$$

only the cubic phase exists.

(ii) For $T_1>T>T_c$, where $T_c=T_0+{\alpha'_{11}}^2/4\alpha_0\alpha_{111}$, there are two solutions:

$$\text{(a)} \quad P_i=0, \quad \eta_{ij}=0 \quad (i,j=1,2,3) \tag{3.7}$$

and

$$\text{(b)} \quad \mathbf{P}=(\pm P_0,0,0),(0,\pm P_0,0),(0,0,\pm P_0) \tag{3.8}$$

with

$$P_0=\left[\frac{-\alpha'_{11}+({\alpha'_{11}}^2-3\alpha_1\alpha_{111})^{1/2}}{3\alpha_{111}}\right]^{1/2} , \tag{3.9}$$

$$\eta_{\parallel}=\frac{P_0^2}{3}\left[\frac{\hat{q}_{11}}{\hat{C}_{11}}+\frac{2\hat{q}_{22}}{\hat{C}_{22}}\right] , \tag{3.10}$$

$$\eta_{\perp}=\frac{P_0^2}{3}\left[\frac{\hat{q}_{11}}{\hat{C}_{11}}-\frac{\hat{q}_{22}}{\hat{C}_{22}}\right] , \tag{3.11}$$

$$\eta_{ij}=0 \quad (i\neq j) . \tag{3.12}$$

Here $\eta_{\parallel}$ and $\eta_{\perp}$ are the normal strain components in the directions parallel and perpendicular to the tetragonal axis in each of the three tetragonal states, respectively.

Solution (a) represents a thermodynamically stable cubic phase and (b) indicates that an additional tetragonal metastable phase also exists in this temperature region. This metastable phase can be stabilized to become the ferroelectric phase with further cooling. T_c is the phase-transition temperature at which the free energies of the cubic and tetragonal phases are equal.

(iii) For $T_c\geq T>T_0$, solutions (a) and (b) in (ii) exist, but in this temperature region the tetragonal phase becomes thermodynamically stable and the cubic phase becomes metastable.

(iv) For $T<T_0$, only the tetragonal phase exists [solutions (b) in (ii)].

IV. 180° TWIN SOLUTION

Twinning exists because of the coexistence of several energetically degenerate variants in the low-temperature phase. The domain wall represents a transition region between two tetragonal variants, where the lattice structure is distorted, so that the formation of domain walls introduces inhomogeneity to the system. The 180° twins represent one kind of inhomogeneous structure, which consists of two variants whose polarizations are 180° out of phase. The tetragonal axes of these two domains are the same. A continuous space profile of a 180° twin can be obtained by solving Eqs. (3.1)–(3.3) under specified boundary conditions. Taking, for example, the two variants $(0,0,\pm P_0)$ to form a [100] 180° twin, the boundary conditions are

$$\lim_{x_1\to\pm\infty} P_3(x_1)=\pm P_0 , \tag{4.1}$$

$$\lim_{x_1\to\pm\infty} \sigma_{ij}^{\text{tot}}(x_1)=0 \quad \text{for } ij=11,22,33 , \tag{4.2}$$

$$\sigma_{ij}^{\text{tot}}(x_1)=0 \quad \text{for } ij=23,13,12 . \tag{4.3}$$

Here Eq. (4.1) states that the polarization component $P_3(x_1)$ should match one of the two values corresponding to the two variants far from the domain wall; Eqs. (4.2) and (4.3) represent, respectively, that the system is free from mechanical stresses in the homogeneous region ($|x_1|\to\infty$) and there are no shear stresses in the entire system.

We assume a Q1D solution exists and make the following ansatz for the primary and secondary order parameters,

$$\mathbf{P}=(0,0,P_3(x_1)) , \tag{4.4}$$

$$\eta_{ij}=\eta_{ij}(x_1) . \tag{4.5}$$

Substituting Eqs. (4.4) and (4.5) into Eqs. (3.1)–(3.3) generates a second-order nonlinear differential equation for $P(x_1)$

$$2\alpha_1^+P_3+4\alpha_{11}^+P_3^3+6\alpha_{111}P_3^5-g_{11}P_{3,11}=0 \tag{4.6}$$

with

$$\alpha_1^+=\alpha_1-\left[\frac{\hat{C}_{22}}{C_{11}}q_{12}\eta_{\perp}+\left[q_{11}-\frac{C_{12}}{C_{11}}q_{12}\right]\eta_{\parallel}\right] , \tag{4.7}$$

$$\alpha_{11}^+=\alpha_{11}-\frac{q_{12}^2}{2C_{11}} . \tag{4.8}$$

Equation (4.6) has a kink solution[15] which satisfies the boundary condition (4.1)

$$P_3(x_1)=\frac{P_0\sinh(x_1/\xi_{180})}{[A+\sinh^2(x_1/\xi_{180})]^{1/2}}\ , \tag{4.9}$$

where $\sinh(y)$ is the hyperbolic sine function and

$$\xi_{180}=\frac{\sqrt{g_{11}}}{P_0(6\alpha_{111}P_0^2+2\alpha_{11}^+)^{1/2}}\ , \tag{4.10a}$$

$$A=\frac{(3\alpha_{111}P_0^2+\alpha_{11}^+)}{(2\alpha_{111}P_0^2+\alpha_{11}^+)}\ . \tag{4.10b}$$

The elastic strain field associated with the 180° twin solution can be derived from Eqs. (3.2) and (3.3) together with the Q1D solution (4.9),

$$\eta_{22}=\eta_\perp\ , \tag{4.11a}$$

$$\eta_{33}=\eta_\parallel\ , \tag{4.11b}$$

$$\eta_{11}=\eta_\perp-\frac{q_{12}}{C_{11}}\frac{P_0^2}{1+A^{-1}\sinh^2(x_1/\xi_{180})}\ , \tag{4.11c}$$

$$\eta_{12}=0\ , \tag{4.11d}$$

$$\eta_{13}=0\ , \tag{4.11e}$$

$$\eta_{23}=0\ . \tag{4.11f}$$

The kink solution (4.9) gives the continuous space profile of polarization for a 180° twin in the tetragonal phase. A planar domain wall which bridges the $(0,0,-P_0)$ and $(0,0,P_0)$ states is located at $x_1=0$ in our coordinate system. Note that the strain components Eqs. (4.11a)–(4.11f) were derived under the assumption that the twin structure is free of defects, i.e., the distortion caused by the presence of a domain wall is purely displacive, no atoms are lost or gained in forming the twin. It can be seen from Eqs. (4.11a)–(4.11f) that all the strain components of a twin structure are the same as those for a single domain tetragonal system except η_{11} [Eq. (4.11c)]. In other words, the distortion caused by the Q1D domain wall is only in the x_1 direction. The displacement $\mathbf{u}$ with respect to the cubic structure can be easily integrated from Eqs. (4.11a)–(4.11d),

$$\mathbf{u}=\begin{bmatrix}\eta_\perp x_1+\Delta u\\ \eta_\perp x_2\\ \eta_\parallel x_3\end{bmatrix} \tag{4.12}$$

with

$$\Delta u=-\frac{q_{12}}{C_{11}}P_0^2\xi_{180}\xi_1\operatorname{arctanh}\left[\frac{1}{\xi_1}\tanh(x_1/\xi_{180})\right]\ , \tag{4.13}$$

$$\xi_1=\left[3+\frac{\alpha_{11}^+}{\alpha_{11}P_0^2}\right]^{1/2}\ . \tag{4.14}$$

Since the electrostrictive constant q_{12} is usually negative, there is an expansion in the x_1 dimension associated with the 180° wall, with the amount of

$$\Delta L_1=-2\frac{q_{12}}{C_{11}}\xi_1\xi_{180}\operatorname{arctanh}\left[\frac{1}{\xi_1}\right]\ . \tag{4.15}$$

It was proved[11] that the dimensional changes are correlated under the elastic compatibility constraints, Eq. (3.3). Therefore, in order to sustain the displacive change in the x_1 direction without affecting the other two dimensions, we need to apply inhomogeneous stresses on the lateral surfaces; these required stresses are

$$\sigma_{22}^{\rm tot}=\frac{(\hat{C}_{22}/C_{11})q_{12}P_0^2}{1+A^{-1}\sinh^2(x_1/\xi_{180})}\ , \tag{4.16}$$

$$\sigma_{33}^{\rm tot}=\frac{[q_{11}-(C_{12}/C_{11})q_{12}]P_0^2}{1+A^{-1}\sinh^2(x_1/\xi_{180})}\ . \tag{4.17}$$

It is interesting to compare the 180° twin solution here with the antiphase solution obtained in Ref. 16. Although the forms representing the coupling between the order parameter and the elastic strain were taken to be identical (determined by the cubic symmetry) in the two cases, the underlying physics is different. For the antiphase solution, the rotation axes of the octahedra are the same in the two domains divided by an antiphase boundary, which implies that the tetragonal axis must be perpendicular to the antiphase boundary plane; but, for the 180° ferroelectric twin discussed here, charge neutrality is a prerequisite to ensure a stable static configuration, which means that the polarization vectors and, hence, the tetragonal axes of the two domains are parallel to the twin boundary plane. As a consequence of this difference, the normal-surface stresses required in the two lateral directions for supporting the Q1D solutions become distinct for the 180° ferroelectric twin but are the same for the antiphase solution. Another obvious difference between the two cases is the functional form of the order-parameter profile: a ϕ^4-type kink (second-order phase transition) in Ref. 16 but a ϕ^6-type kink (first-order phase transition) in this paper. In addition, since the coupling constants q_{11} and q_{12} (B_1 and B_2 in Ref. 16) have opposite sign, the antiphase boundary induces shrinkage but the 180° twin boundary causes expansion in the dimension along the twin (antiphase) boundary normal.

There is a certain amount of energy stored in the 180° domain wall. We define the energy density per unit area for a single domain wall to be $E_{180°}$, which is a function of temperature only and is given by

$$E_{180°}=\int_{-\infty}^{\infty}(F-F_0)dx_1\ . \tag{4.18}$$

Here F_0 is the energy density of a homogeneous system at a given temperature. The integration of Eq. (4.18) can be carried out by substituting the solutions (4.9)–(4.11) into Eq. (2.1). After some algebra, a closed form can be obtained,

$$E_{180°}=\left[\frac{2g_{11}}{\alpha_{111}}\right]^{1/2}\left[\frac{\alpha_{11}^+}{2}P_0\left[3P_0^2+\frac{\alpha_{11}^+}{\alpha_{111}}\right]^{1/2}-\left[\frac{\alpha_{11}^{+2}}{4\alpha_{111}}-\alpha_1^+\right]\operatorname{arcsinh}\frac{P_0}{(2P_0^2+\alpha_{11}^+/\alpha_{111})^{1/2}}\right]\ . \tag{4.19}$$

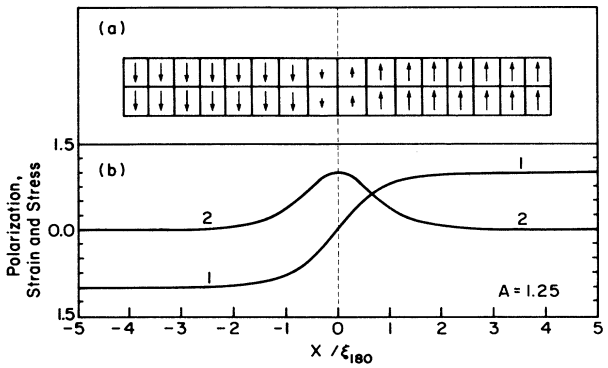

FIG. 1. 180° twin solution. (a) Illustration of polarization and unit-cell distortion in a 180° twin structure represented by a continuum solution. (b) Space profile of normalized polarization P/P_0 (curve 1) and normalized inhomogeneous components of strain $-(C_{11}/q_{12}P_0^2)(\eta_{11}-\eta_\perp)$, and stresses $(C_{11}/\hat{C}_{22}q_{12}P_0^2)\sigma_{22}^{\rm tot}$ and $[q_{11}-(C_{12}/C_{11})q_{12}]^{-1}P_0^{-2}\sigma_{33}^{\rm tot}$ (curve 2).

For $T<T_c$, $E_{180°}$ is positive definite (see arguments below), so that a twin structure has higher energy compared to a single domain structure. As mentioned above, external constraints are needed to stabilize base twin solution; these are often provided by surface stresses or intergranular interaction in a polycrystal (or ceramic) system. It should be pointed out that defects play a very important role in stabilizing the twin structures in a real system, but it is beyond the scope of this paper.

In Fig. 1(b) are plots of polarization, strain, and stress profiles in dimensionless form, each physical quantity has been rescaled with a different scaling factor. The polarization and unit-cell distortion represented by the solutions are illustrated in Fig. 1(a).

V. 90° TWIN SOLUTION

The other type of stable twin structure in the tetragonal phase besides the 180° twin is the 90° twin, which consists of two domains whose tetragonal axes (or polarizations) are (almost) perpendicular to each other. Since the twin structure with charged twin boundary (with polarizations head-to-head or tail-to-tail) has additional Coulomb energy, only the twin structure with charge neutral boundary (head-to-tail configuration) is a stable configuration for the 90° twin.

We consider a twin structure of the two following variants: $\mathbf{P}_1=(P_0,0,0)$ and $\mathbf{P}_2=(0,P_0,0)$, with the twin boundary oriented in [110]. It is convenient to work in a new coordinate system (s,r,x_3) which is a 45° rotation of the x_1-x_2 plane around x_3. The two coordinate systems, the structure and the polarization configurations, are shown in Fig. 2. We choose a system with its dimension along the s coordinate much larger than the other dimensions in order to set up the boundary conditions $(L_s\sim\infty\gg L_r,L_3)$, and assume that the space profile of the polarization vector of the system is quasi-one-dimensional, i.e., it depends on the space variable s only. Our goal is to seek solution of the kind $\mathbf{P}=[P_1(s),P_2(s),0]$ for the 90° twin structure, which satisfies the boundary conditions

$$\lim_{s\to-\infty}\mathbf{P}=(P_0,0,0)$$

and

$$\lim_{s\to+\infty}\mathbf{P}=(0,P_0,0)\ .$$

In order to use this Q1D nature to our advantage, we will convert all quantities into the new coordinate system, the polarization becomes $\mathbf{P}=[P_s(s),P_r(s),0]$, and the free energy of this 90° twin can be written as

$$F_{90°}=\alpha_1(P_s^2+P_r^2)+\alpha_{11}(P_s^2+P_r^2)^2+\frac{\alpha_{12}}{4}(P_s^2-P_r^2)^2+\alpha_{111}(P_s^2+P_r^2)^3+\frac{\alpha_{112}-3\alpha_{111}}{4}(P_s^4-P_r^4)(P_s^2-P_r^2)$$
$$+\frac{G_{ss}}{2}P_{s,s}^2+\frac{G_{rs}}{2}P_{r,s}^2+F_{\rm el}(\eta_{kl})+F_c(P_s,P_r,\eta_{kl})\quad(k,l=r,s,x_3)\ , \tag{5.1}$$

where

$$G_{ss}=(g_{11}+g_{12}+2g_{44})/2\ , \tag{5.2a}$$

$$G_{rs}=(g_{11}-g_{12})/2\ , \tag{5.2b}$$

$F_{\rm el}(\eta_{kl})$ and $F_c(P_s,P_r,\eta_{kl})$ are the elastic and coupling energies [Eqs. (2.3) and (2.4)], respectively, in the new coordinate system.

The boundary conditions as $s\to\pm\infty$ are, for the polarization and strain components, respectively,

$$\lim_{s\to\pm\infty}P_s=\frac{P_0}{\sqrt{2}}\ , \tag{5.3a}$$

$$\lim_{s\to\pm\infty}P_r=\pm\frac{P_0}{\sqrt{2}}\ , \tag{5.3b}$$

$$\lim_{s\to\pm\infty}\eta_{rr}=\lim_{s\to\pm\infty}\eta_{ss} \tag{5.3c}$$

$$=(\eta_\parallel+\eta_\perp)/2\ , \tag{5.3d}$$

$$\lim_{s\to\pm\infty}\eta_{sr}=\pm(\eta_\parallel-\eta_\perp)/2\ . \tag{5.3e}$$

In addition, there should be no mechanical constraints in the single domain states $(s\to\pm\infty)$ and no shear stress in the x_3 direction. These arguments lead to the mechanical boundary conditions

$$\lim_{s\to\pm\infty}\sigma_{ij}^{\rm tot}(s)=0\quad(i,j=r,s,x_3)\ , \tag{5.4}$$

$$\sigma_{s3}=\sigma_{r3}=0\ . \tag{5.5}$$

The compatibility relations (3.3) give three nontrivial

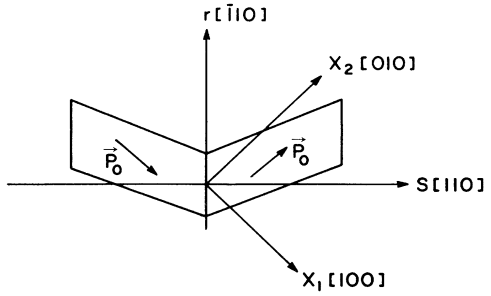

FIG. 2. (001) cross section of a 90° twin crystal with a twin boundary at $s=0$. The orientation of the new and old axes are shown in the figure, and the directions of the polarizations in the two domains are also indicated.

constraints for the twin solution. They are, in the new coordinate system,

$$\eta_{rr,ss}=0 , \tag{5.6a}$$

$$\eta_{33,ss}=0 , \tag{5.6b}$$

$$\eta_{rs,ss}=0 . \tag{5.6c}$$

These equations (5.6a)–(5.6c) together with the boundary conditions (5.3) and (5.5), can determine four of the six independent strain components; they are

$$\eta_{r3}=\eta_{s3}=0 , \tag{5.7a}$$

$$\eta_{rr}=\tfrac{1}{2}(\eta_{\parallel}+\eta_{\perp}) , \tag{5.7b}$$

$$\eta_{33}=\eta_{\perp} . \tag{5.7c}$$

These four components are constants in space since the quantities $\eta_{\parallel}$ and $\eta_{\perp}$ are functions of temperature only. The other two of the six independent strain components are inhomogeneous and strongly coupled to the primary order parameter. From Eq. (3.2) and the boundary conditions (5.4), we have

$$\eta_{rs}=(\hat{q}_{22}/\hat{C}_{22})P_sP_r , \tag{5.8}$$

$$\eta_{ss}=\tfrac{1}{2}(\eta_{\parallel}+\eta_{\perp}) -\frac{1}{2C_{ss}}\{(q_{11}+q_{12})[P_0^2-(P_s^2+P_r^2)] -q_{44}(P_s^2-P_r^2)\} , \tag{5.9a}$$

where

$$C_{ss}=\frac{C_{11}+C_{12}}{2}+C_{44} . \tag{5.9b}$$

By using these strain solutions and the definitions of $\eta_{\parallel}$ and $\eta_{\perp}$, we can explicitly write the equilibrium conditions (3.1) in the rotated coordinate system:

$$G_{ss}P_{s,ss}=2\alpha_1^sP_s+4\alpha_{11}^sP_s^3+4\alpha_{11}^{sr}P_sP_r^2 +\tfrac{3}{2}(\alpha_{111}+\alpha_{112})P_s^5+(15\alpha_{111}-\alpha_{112})P_s^3P_r^2 +\tfrac{1}{2}(15\alpha_{111}-\alpha_{112})P_sP_r^4 , \tag{5.10a}$$

$$G_{rs}P_{r,ss}=2\alpha_1^rP_r+4\alpha_{11}^rP_r^3+4\alpha_{11}^{sr}P_rP_s^2 +\tfrac{3}{2}(\alpha_{111}+\alpha_{112})P_s^5+(15\alpha_{111}-\alpha_{112})P_r^3P_s^2 +\tfrac{1}{2}(15\alpha_{111}-\alpha_{112})P_rP_s^4 , \tag{5.10b}$$

where

$$\alpha_1^s=\alpha_1-\left[\frac{1}{3}\frac{\hat{q}_{11}^2}{\hat{C}_{11}}+\frac{1}{6}\frac{\hat{q}_{22}^2}{\hat{C}_{22}} -\frac{(q_{11}+q_{12})(q_{11}+q_{12}+q_{44})}{4C_{ss}}\right]P_0^2 , \tag{5.11a}$$

$$\alpha_1^r=\alpha_1-\left[\frac{1}{3}\frac{\hat{q}_{11}^2}{\hat{C}_{11}}+\frac{1}{6}\frac{\hat{q}_{22}^2}{\hat{C}_{22}} -\frac{(q_{11}+q_{12})(q_{11}+q_{12}-q_{44})}{4C_{ss}}\right]P_0^2 , \tag{5.11b}$$

$$\alpha_{11}^s=\alpha_{11}+\frac{\alpha_{12}}{4}-\frac{(q_{11}+q_{12}+q_{44})^2}{8C_{ss}} , \tag{5.11c}$$

$$\alpha_{11}^r=\alpha_{11}+\frac{\alpha_{12}}{4}-\frac{(q_{11}+q_{12}-q_{44})^2}{8C_{ss}} , \tag{5.11d}$$

$$\alpha_{11}^{sr}=\alpha_{11}-\frac{\alpha_{12}}{4}-\frac{(q_{11}+q_{12})^2-q_{44}^2}{8C_{ss}}-\frac{\hat{q}_{22}}{2\hat{C}_{22}} . \tag{5.11e}$$

In general, Eqs. (5.10a) and (5.10b) have to be solved numerically. All the coefficients may be determined from dielectric, electrostrictive, and elastic measurements, and from phonon dispersion curves for a given system. We will show this numerical procedure elsewhere.[12]

Putting the quantitative individual characters of each specific system aside in the following, we will abstract the common features of a 90° twin solution by choosing some of the parameters to special values. For instance, if

$$\alpha_{11}^{sr}=0 , \tag{5.12}$$

$$15\alpha_{111}=\alpha_{112} , \tag{5.13}$$

then we can obtain analytic solutions for P_s and P_r from Eqs. (5.10a) and (5.10b),

$$P_s=\frac{1}{\sqrt{2}}P_0 , \tag{5.14a}$$

$$P_r=\frac{1}{\sqrt{2}}P_0\frac{\sinh(s/\xi_{90})}{[B+\sinh^2(s/\xi_{90})]^{1/2}} , \tag{5.14b}$$

where

$$\xi_{90}=\frac{1}{P_0}\left[\frac{G_{rs}}{6\alpha_{111}P_0+\alpha_{11}^r}\right]^{1/2} . \tag{5.15a}$$

$$B=\frac{6\alpha_{111}P_0^2+\alpha_{11}^r}{4\alpha_{111}P_0^2+\alpha_{11}^r} . \tag{5.15b}$$

The two inhomogeneous strain components, Eqs. (5.8) and (5.9), now become

$$\eta_{rs}=(\hat{q}_{22}/2\hat{C}_{22})P_0^2\frac{\sinh(s/\xi_{90})}{[B+\sinh^2(s/\xi_{90})]^{1/2}}\ , \tag{5.16a}$$

$$\eta_{ss}=\tfrac{1}{2}(\eta_{\parallel}+\eta_{\perp}) -\frac{P_0^2}{4C_{ss}}(q_{11}+q_{12}-q_{44})\frac{1}{1+B^{-1}\sinh^2(s/\xi_{90})}\ . \tag{5.16b}$$

Equation (5.16a) describes the shape change (or bending) caused by the 90° twinning and Eq. (5.16b) indicates a dimensional change in the s direction with the total amount of

$$\Delta L_s=-\frac{\xi_{90}P_0^2}{2C_{ss}}(q_{11}+q_{12}-q_{44}) \times\left[\frac{B}{B-1}\right]^{1/2}\ln(\sqrt{B}+\sqrt{B-1})\ . \tag{5.17}$$

Note the mathematical forms of Eqs. (4.15) and (5.17) are interconvertible. The two position-dependent normal strain components, which are required to support the Q1D solution, are given by

$$\sigma_{rr}^{\rm tot}=\frac{P_0^2}{4C_{ss}}[2C_{44}(q_{11}+q_{12})+(C_{11}+C_{12})q_{44}] \times\frac{1}{1+B^{-1}\sinh^2(s/\xi_{90})}\ , \tag{5.18a}$$

$$\sigma_{33}^{\rm tot}=\frac{P_0^2}{4C_{ss}}[-C_{44}(q_{11}-q_{44})+(C_{11}+2C_{44})q_{12}] \times\frac{1}{1+B^{-1}\sinh^2(s/\xi_{90})}\ . \tag{5.18b}$$

Similar to Eqs. (3.18) and (3.19), the energy density stored in this 90° domain wall can be obtained from the analytic solution, (5.14a) and (5.14b),

$$E_{90^\circ}=\left[\frac{G_{rs}}{2\alpha_{111}}\right]^{1/2}\left[\frac{\alpha_{11}^r P_0}{4}\left[3P_0^2+\frac{\alpha_{11}^r}{2\alpha_{111}}\right]^{1/2}-\left[\frac{\alpha_{11}^2}{16\alpha_{111}}-\alpha_1^r\right]\operatorname{arcsinh}\frac{P_0}{(2P_0^2+\alpha_{11}^r/2\alpha_{111})^{1/2}}\right]\ . \tag{5.19}$$

For a static configuration, $E_{90^\circ}>0$, which may not be obvious from Eq. (5.19) but can be proved to be true for more general cases. According to definition we can write the energy density of the 90° domain wall as

$$E_{90^\circ}=\int_{-\infty}^{\infty}[F(P_i,P_{i,j})-F_L(P_0)]ds =2\int_{-\infty}^{\infty}[F_L(P_i)-F_L(P_0)]ds\ . \tag{5.20}$$

Here Eqs. (5.10a) and (5.10b) have been used, $F_L(P_i)$ is the Landau energy which has a minimum value $F_L(P_0)$ for $T<T_c$, i.e., $F_L(P_i)>F_L(P_0)$ for $P_i\neq P_0$, therefore the integral in Eq. (5.20) is a positive value, hence, $E_{90^\circ}>0$. The same argument also applies to E_{180° obtained in Sec. IV.

Figure 3(a) illustrates the 90° ferroelectric twin structure and the associated elastic distortion. In the twin boundary region, not only the rotation of polarization vector occurs, the magnitude of the polarization also changes in space as shown in Fig. 3(b). For the special choice of parameters, Eqs. (5.12) and (5.13), the magnitude of polarization is

$$|P|=P_0\left[\frac{(B/2)+\sinh(s/\xi_{90})}{B+\sinh(s/\xi_{90})}\right]^{1/2}\leq P_0\ , \tag{5.21}$$

which is less or equal to the polarization in the single-phase region. For other choices of the parameters, or in real system, Eq. (5.21) may not be true.

VI. SUMMARY AND CONCLUSIONS

Based on Landau-Ginzburg theory, a continuum model has been developed for the twin structure in tetragonal

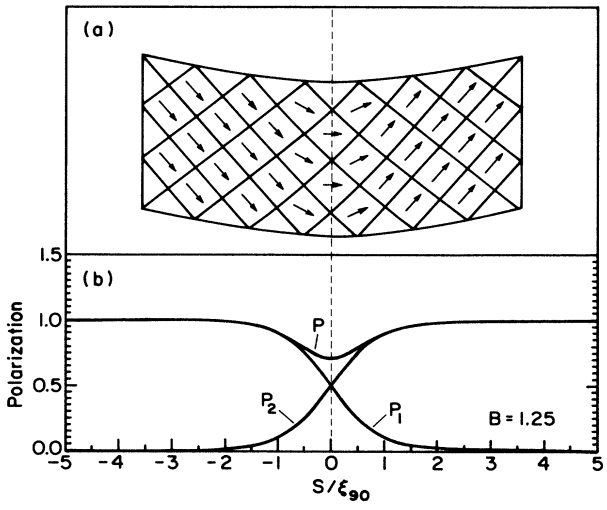

FIG. 3. 90° twin solution. (a) Illustration of the polarization variation and unit-cell distortion. (b) Space profiles of the normalized polarization components P_1, P_2, and the magnitude P, the parameters have been set to satisfy Eqs. (5.12) and (5.13).

ferroelectric perovskites, which is a three-dimensional ϕ^6 model with the primary order parameter chosen to be the material measure of polarization. Under the assumption of a coherent interface, the model can describe the O_h-C_{4v} first-order proper ferroelectric phase transition and gives rise to the space profiles of a 180° twin and a 90° twin with charge-neutral twin boundary.

The ferroelectric phase transitions are often accompanied by unit-cell distortions (in certain cases the distortions could be very large); therefore, a proper ferroelectric is usually an improper ferroelastic. The second-order improper ferroelastic phase transition has been addressed in Ref. 16; that model can also describe a second-order ferroelectric phase transition with proper physical constraints, such as the orientational relationship between tetragonal axes of domains and the twin boundary. For the same reason, the ferroelectric ϕ^6 model developed in this paper may also be generalized to describe other improper ferroelastic systems.

It is interesting to see that the coupling of the order parameter to strain has different effects in the case of second-order and first-order phase transitions.[11,17] The transition temperature is the same for the former, but will be shifted for the latter resulting from this coupling and the imposed boundary conditions.

Due to the nonlocal coupling of the polarization, the domain walls acquire finite width. In addition, as shown in Fig. 3(a), the crystallographic symmetry is lower in the 90° domain-wall region. At the domain-wall center, the structure is quasiorthorhombic, which implies that the 90° domain walls are natural nucleation sites for the tetragonal-orthorhombic transition if the orthorhombic phase happens to be the next low-temperature thermodynamically stable phase.

We have also proved in Sec. V that both 180° and 90° domain walls contain positive energy, so that the existence of a stable Q1D twin structure must be supported by either inhomogeneous (internal or external) stress distribution or by defects. In a ceramic system the stresses are provided by intergranular coupling. This implies that the stress concentration at the grain boundaries is inhomogeneous.

An important application of any ferroelectric material is based on its piezoelectric effect. Strictly speaking, the macroscopic piezoelectric effect comes from two different origins: For a single domain single crystal, the induced strain is due to the direct coupling of the polarization to the unit-cell distortion, which, in our case, is proportional to the square of polarization. Therefore, the intrinsic piezoelectric constants are proportional to the product of the electrostrictive constants and the components of spontaneous polarization. For a multidomain system, such as a ceramic, there are additional contributions from the motion of 90° domain walls, which can be understood from Fig. 3(a). We can clearly see a shape change associated with the misalignment of polarization vectors in the two domains. A lattice movement of an entire domain in the direction parallel to the twin boundary plane can be generated by the motion of a 90° domain wall along its normal direction. We define this additional piezoelectric effect as the "orientational effect," it is extrinsic in nature. The strength of this effect is determined by the degree of unit-cell distortion (relative to the cubic structure) and the maximum distance which a domain wall can move without breaking the atomic coherency. Except in a single domain single crystal, these two effects exist simultaneously and interact with each other. In order to analyze this complicated process, one must know the detailed structure in the domain-wall region, which is one of the achievements of the present work. We will show in a forthcoming paper[12] how to determine those expansion coefficients from experiments so as to quantify the atomic displacements in a ferroelectric twin structure for a specific system.

ACKNOWLEDGMENTS

We are indebted to Professor G. R. Barsch for suggesting the approach to this project and for providing close guidance during the initial phases of this work. This research was supported by the Office of Naval Research under Grant No. N00014-89-J-1689.

[1]M. E. Lines and A. M. Glass, *Principles and Applications of Ferroelectrics and Related Materials* (Clarendon, Oxford, 1979).

[2]E. K. W. Goo, R. K. Mishra, and G. Thomas, J. Appl. Phys. **52**, 2939 (1981).

[3]P. G. Lucuta and V. Teodoresu, Appl. Phys. A **37**, 237 (1985).

[4]Von Cieminski, C. Kleint, H. Beige, and R. Hoche, Ferroelectrics **109**, 95 (1990).

[5]L. Pardo, J. Mendida, A. Gonzalez, and J. De. Frutos, Ferroelectrics **94**, 189 (1990).

[6]G. Arlt, Ferroelectrics **76**, 451 (1987).

[7]C. A. Randall, D. J. Barber, and R. W. Whatmore, J. Mater. Sci. **22**, 925 (1987).

[8]V. A. Zhirnov, Zh. Eksp. Teor. Fiz. **35**, 1175 (1958) [Sov. Phys. JETP **35**, 822 (1959)].

[9]I. I. Ivanchik, Fiz. Tverd. Tela (Leningrad) **3**, 3731 (1961) [Sov. Phys. Solid State **3**, 2705 (1962)].

[10]L. N. Bulaevskii, Fiz. Tverd. Tela (Leningrad) **5**, 3183 (1963) [Sov. Phys. Solid State **5**, 2329 (1964)].

[11]W. Cao, G. R. Barsch, and J. A. Krumhansl, Phys. Rev. B **42**, 6396 (1990).

[12]W. Cao (unpublished).

[13]G. R. Barsch, B. N. N. Achar, and L. E. Cross, Ferroelectrics **35**, 187 (1981).

[14]E. A. N. Love, *A Treatise on the Mathematical Theory of Elasticity* (Dover, New York, 1944), p. 49.

[15]F. Falk, Z. Phys. B **51**, 177 (1983).

[16]W. Cao and G. R. Barsch, Phys. Rev. B **41**, 4334 (1990).

[17]J. Lajzerowicz, Ferroelectrics **35**, 219 (1981).